High-Density Layer at the SiO_2/Si Interface Observed by Difference X-Ray Reflectivity

Jpn. J. Appl. Phys. Vol. 35 (1996) pp. L 67–L 70
Part 2, No. 1B, 15 January 1996

High-Density Layer at the SiO_2/Si Interface Observed by Difference X-Ray Reflectivity

Naoki AWAJI, Satoshi OHKUBO, Toshiro NAKANISHI, Yoshihiro SUGITA,
Kanetake TAKASAKI and Satoshi KOMIYA
Fujitsu Laboratories Ltd., 10-1 Morinosato-Wakamiya, Atsugi 243-01, Japan

(Received October 26, 1995; accepted for publication November 29, 1995)

We have developed a high-accuracy difference X-ray reflectivity (DXR) method using intense synchrotron radiation for the evaluation of ultrathin thermal oxides on Si(100). By carefully analyzing DXR data for gate oxides with thicknesses of 40 Å and 70 Å grown at 800°C to 1000°C, the existence of a dense (~2.4 g/cm^3), thin (~10 Å) layer at the SiO_2/Si interface has been revealed. The thickness of the interfacial layer decreases with increasing oxidation temperature. Oxides grown in O_3 or HCl/O_2 have a thinner interfacial layer compared to those grown in O_2.

KEYWORDS: X-ray reflectivity, gate oxide, interfacial layer, SiO_2/Si interface, film density, synchrotron radiation

The current trend toward increased density of ultralarge-scale integrated devices has required highiy reliable ultrathin SiO_2 gates as thin as 40 Å. For such ultrathin oxides, characterization of the initial surface before oxidation is an important issue along with the interfacial structure of the grown oxide. In the previous paper,[1,2] we developed high-accuracy X-ray reflectivity techniques using intense synchrotron radiation for the evaluation of native oxides formed by various chemical treatments. In this work, we generalized the method as a difference X-ray reflectivity technique and applied this to evaluate the structure of ultrathin thermally grown oxides.

We prepared thermal oxides with the thicknesses of 40 Å and 70 Å. Czochralski (CZ) grown Si (100) wafers were cleaned by H_2SO_4/H_2O_2 followed by dipping in 5% HF solution to remove chemically formed oxides. These wafers were then treated in boiled HNO_3 solution to form native oxide. For the preparation of 40 Å oxides, part of the wafers were treated with UV/O_3 prior to the oxidation to elucidate the effect of the quality of native oxide on the grown oxide. The UV/O_3 treatment was performed by transferring the wafer in a quartz chamber, in which a highly purified oxygen gas containing 5% ozone produced by a discharge ozonizer flows (2SLM), with irradiation from a mercury tube for 5 minutes.[3] These wafers were transferred to the load-locked oxidation furnace without exposure to air to avoid humidity and contamination. Oxides 40 Å thick were grown at 800°C in 200 Torr O_3 ambient, and better electric properties were obtained compared to using O_2 ambient. The heating system is a hot-walled type with 4–5% ozone generated by a discharge ozonizer. We grew 70-Å-thick oxides in three different ambients, 200 Torr O_2 200 Torr O_3 and atmospheric-pressure HCl/O_2, at temperatures between 800°C and 1000°C to elucidate their structural differences.[4]

The X-ray reflectivity was measured using synchrotron radiation at the beamline 17C photon factory (PF) KEK, by selecting the X-ray wavelength of 1.3 Å. In the previous analysis, we extracted the contribution of native oxide by subtracting log-reflectivity of the Si substrate from that of native oxides for accurate evaluation. Here, we generalize the subtracted reflectivity as DXR (denoted by ΔR) defined as

$$\Delta R = \log_{10}(R/R_{\mathrm{ave}}),$$

where R_{ave} is the reference reflectivity that reproduces the average behavior of the measured reflectivity, R. R_{ave} must be clearly defined and has no oscillatory behavior. It is not difficult to mathematically confirm, if the densities of film and substrate are similar, reflectivity from the substrate is appropriate for R_{ave}. To obtain DXR of the thermally grown oxides, the measured reflectivity of the Si substrate is not appropriate for R_{ave} since the surface roughnesses of the grown oxide and that of the Si substrate are not necessarily similar, in contrast to the case of native oxide. Therefore, we applied the calculated reflectivity of the Si substrate with the same surface roughness, σ_{SiO_2}, as that of grown oxide for the average reflectivity of $R_{\mathrm{ave}} = R_{\mathrm{Si,calc}}(\sigma_{SiO_2})$.

We developed an optimization program based on the Marquardt minimization procedure for the extraction of film parameters, where the reflectivity is calculated based on the Vidal and Vincent formalism.[5] The following standard error function was applied in the optimization since R_{ave} terms in the observed and calculated ΔR cancel each other out.

$$\chi^2 = \Sigma(\log_{10} R_{\mathrm{data}} - \log_{10} R_{\mathrm{calc}})^2$$

In the least squares refinement of the model for the thermal oxides, there are two possible solutions having the same interference amplitude in which the oxide density is low or high compared to that of the Si substrates. Figure 1 shows the calculated DXR for the 40-Å-thick oxide whose density varied from 2.15 to 2.5 g/cm^3, along with the usual X-ray reflectivity for oxide with the density of 2.15 g/cm^3. From the figure, the interference fringe clearly changes in phase when the oxide density coincides with that of the Si substrates, 2.33 g/cm^3. Then, the ambiguous solutions of density can be resolved from the shape of the first fringe at around the critical angle, ψ_c, where the peaks indicate denser oxides and dips indicate less dense oxides, compared to the density of Si.

In Figs. 2 and 3, typical DXRs are shown for the 40-Å-thick oxides (a) without and (b) with UV/O_3 pretreatment, (c) for 70-Å-thick oxide grown at 1000°C in O_3 ambient, and (d) for 70-Å-thick oxide grown at 1000°C in HCl/O_2 ambient. Based on the first oscillation of the interference, the densities of oxides (a) and (b) exceed

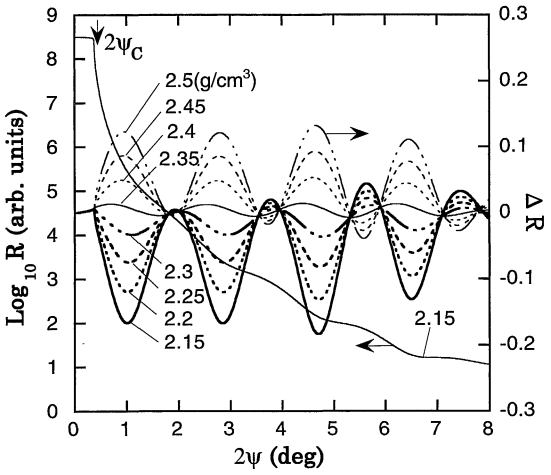

Fig. 1. Calculated difference X-ray reflectivity for 40-Å-thick oxides. The assumed oxide densities are from 2.15 to 2.5 g/cm^3. Interference oscillation changes its phase when the oxide density exceeds that of Si (2.33 g/cm^3). Original X-ray reflectivity for oxide with the density of 2.15 g/cm^3 is also shown.

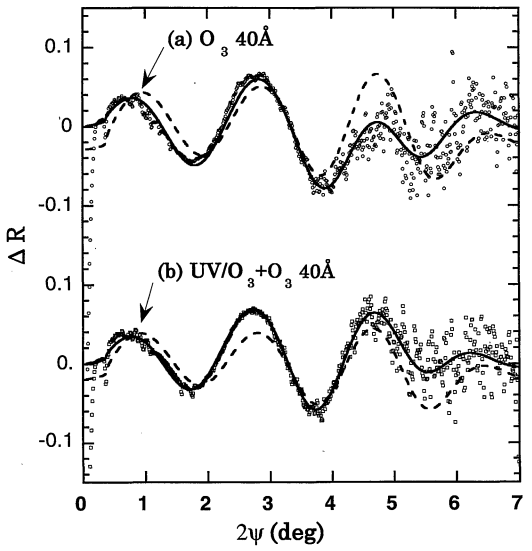

Fig. 2. Observed difference X-ray reflectivity for 40-Å-thick oxides grown at 800°C in O_3 ambient. Before oxidation, (a) Si wafers are cleaned by boiling in HNO_3, and (b) with additional UV/O_3 treatment. Broken lines indicate the results of optimization based on the single-layer model. Solid line represents the two-layer model which assumes a thin, dense interfacial layer at the SiO_2/Si interface.

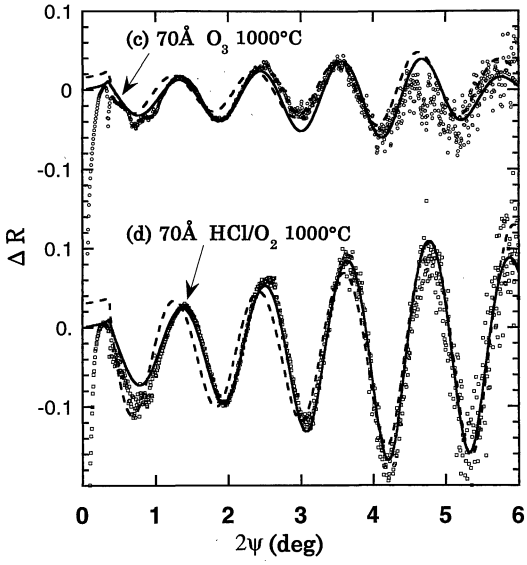

Fig. 3. Observed difference X-ray reflectivity for 70-Å-thick oxides grown at 1000°C in (c) O_3 ambient and (d) HCl/O_2 ambient. Broken line and solid lines are the same as in Fig. 2.

that of Si, whereas oxides (c) and (d) are less dense compared to that of Si.

The broken line in these figures represents the result of the optimization based on the single-layer model where a uniform SiO_2 layer on a Si substrate is assumed. However, the calculated DXR cannot reproduce the measured data, especially the oscillation phase and the intensity modulation. In a highly constrained single-layer model, such intensity modulation and phase change cannot be accommodated. During the analysis, we found that the two-layer model with a thin, high-density interfacial layer precisely reproduces the measured reflectivity, as shown by the solid line in the same figures. The existence of this additional thin layer induces a wide-interval oscillation amplitude with which the regular oscillation from the bulk SiO_2 layer interferes, which can reproduce the observed modulation features. The dense interfacial layer was seen in all measured samples. In the model, we assumed the chemical composition of the interfacial layer to be SiO_2. Results from the X-ray reflectivity technique are insensitive to the chemical composition and chemical bonding. δ in the complex refractive indices, which determines the shape of the reflectivity curve, is given by $(r_0 N_A/2\pi)\lambda^2\rho\,(Z+f')/A$, where r_0 is the classical electron radius, N_A is Avogadro's number, λ is the X-ray wavelength, ρ is the density, A is the atomic mass, and $(Z+f')$ is the atomic scattering factor. In the equation, the composition-dependent electron density $(Z+f')/A$ has values of 0.5040 and 0.5046 for SiO_2 and SiO, respectively, at the X-ray wavelength of 1.3 Å. Since δ is the product of $(Z+f')/A$ and the density, only a 0.12% error can be expected in the estimated density of the interfacial layer whether we assume SiO_2 or SiO for the composition of the layer. In this two-layer model, we set the rms-roughness between the interfacial layer and SiO_2 layer to be 2 Å since the results were insensitive to the roughness. Results from the two-layer model for 40-Å-thick oxides are summarized in Table I. The main difference between these two samples is in the thickness of the interfacial layer, where the UV/O_3 treatment caused the interfacial layer to be 2 Å thinner.

Figure 4 shows the change of the interfacial layer thickness with oxidation temperature for 70-Å-thick samples. The layer thickness ranges from 8 Å to 14 Å and decreases as the temperature increases. The O_2-grown oxides have the thickest interfacial layers, while oxides grown in O_3 and HCl/O_2 ambient have thinner interfacial layers.

Figure 5 shows the densities of the interfacial layer and SiO_2 layer versus oxidation temperature. The density of the interfacial layer is almost constant at around 2.4

Table I. Extracted parameters for 40-Å-thick thermal oxides, grown at 800°C in O_3 ambient, based on the two-layer model where the thin, dense interfacial layer exists at SiO_2/Si interface. σ_s and σ_I indicate the SiO_2 surface roughness and interface roughness at Si substrate, respectively.

Pretreatment before oxidation	Interfacial layer			SiO_2 layer		
	σ_I (Å)	Density (g/cm^3)	Thickness (Å)	σ_s (Å)	Density (g/cm^3)	Thickness (Å)
(a) HNO_3	1.8	2.41	14.0	4.1	2.35	25.6
(b) $HNO_3 + UV/O_3$	2.2	2.41	12.1	4.0	2.36	28.3
Error	±2.0	±0.02	±1.0	±0.1	±0.02	±1.0

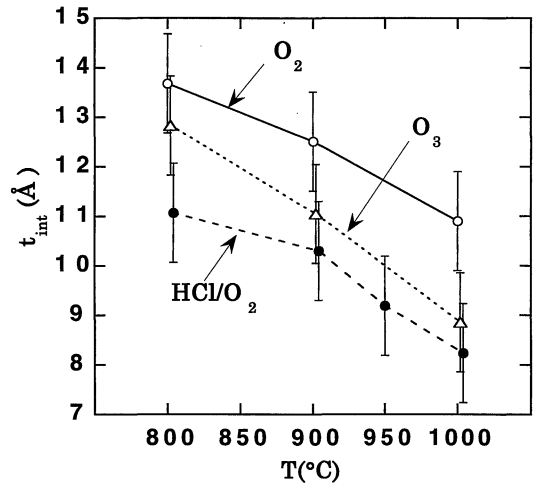

Fig. 4. Change in the thickness of the interfacial layer versus oxidation temperature for 70-Å-thick oxides. Each symbol corresponds to the oxide grown in O_2, O_3 and HCl/O_2 ambients, respectively.

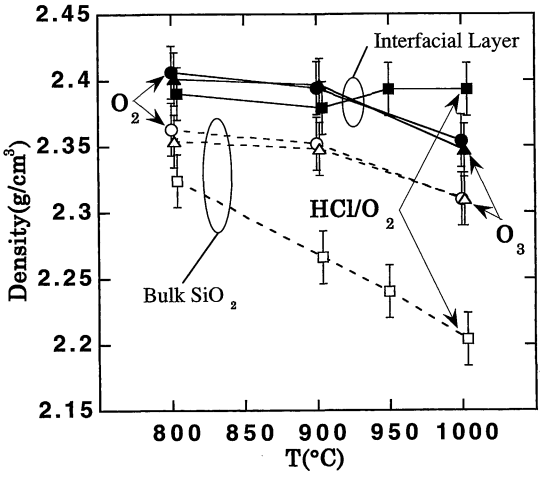

Fig. 5. Evolution of the density of 70-Å-thick oxides on oxidation temperature. Black and white symbols represent the densities of interfacial layer and SiO_2 layer, respectively. Each symbol corresponds to the oxide grown in O_2 and O_3 and HCl/O_2 ambients, respectively.

g/cm^3 for all samples, which indicates the existence of similar oxidation mechanisms even in the HCl/O_2 ambient. On the SiO_2 layer, the density decreases in the same manner as does that of the interfacial layer in the case of O_2 and O_3 oxides, while it decreases much more rapidly in the case of HCl/O_2 oxide as oxidation temperature increases.

The results above, obtained by our X-ray reflectivity technique, clearly contradict those obtained by the grazing-incidence X-ray diffraction technique,[6] where a structure with a 70-Å-thick less dense (2.4 g/cm^3) transition layer between Si and the high-density (2.6 g/cm^3) bulk SiO_2 layer was proposed. However, such a high-density oxide (as dense as quartz) should give the unacceptably high refractive index of 1.55[7] for the optical ellipsometry, compared to the standard value of 1.46. This unacceptably high oxide density with the thick interfacial layer may be due to the large error inherent in the estimation of X-ray penetration depth at incident angles near the critical angle of total reflection.

The density obtained by the DXR method should have small systematic error compared to that in the above method since the observed interference fringes depend on the density difference relative to that of the Si substrate whose density is well known and kept constant at 2.33 g/cm^3 during optimization. The oxide structure, in addition to the effects of thickness and the surface/interface roughness, can be evaluated separately for each sample, since these parameters relate to the interference differently.

So far, various characterizations have been performed on the SiO_2/Si system, and the experimental results have been explained in terms of (I) a model in which the interface is abrupt and has no interfacial layer,[8] (II) a model in which there is a substoichiometric (SiO_x) layer at the SiO_2/Si ihterface,[9,10] (III) a model in which the transition of crystaline Si into amorphous SiO_2 proceeds via the crystalline or ordered phase of SiO_2.[11–14]

Our results clearly disagree with the model I. Also, in the case of model II, the density of the SiO_x layer is unlikely to have a high value compared to the densities of SiO_2 and Si, except in the case of interstitial oxygen diffusion at the interface. In model III, the quasi-stable crystalline polymorph of SiO_2 like tridymite, cristobalite, quartz or coesite are assumed whose densities range from 2.26 to 2.9 g/cm^3 which can account for the observed high density of about 2.4 g/cm^3 of the interfacial layer. Since the unit sizes of these polymorphs are around 6 to 11 Å, the observed thickness of the interfacial layer corresponds to one or two monolayers. Because the crystalline phase will be quasi-stable, the population of the phase will decrease as the oxidation temperature in-

creases, which agrees with the observed decrease in the thickness of the interfacial layer. The existence of chemically active O_3 and HCl accelerates the transition of the crystalline phase into amorphous SiO_2 which leads to a thinner interfacial layer, in agreement with the crystal-truncation rod (CTR) study of O_2- and O_3-grown oxides.[14] Therefore, our results can be explained by model III in which the ordered phase exists near the interface.

The electrical study of 40 Å gate oxides[3] indicated that oxide grown from the UV/O_3-treated dense native oxide has low surface state density (D_{it}) and small leakage current compared to that without the treatment, even under the same oxidation conditions. UV/O_3-treated native oxide, free of poor-quality areas associated with Si–H or Si–OH bonds, generates a uniform oxidation layer at the Si surface whose uniformity remains on the interface in the case of such ultrathin oxides. This may lead to good-quality gate oxides.

O_3-grown oxide has superior electrical properties compared to O_2-grown oxides.[4] It is plausible that ozone accelerates the phase transition of crystal-to-amorphous SiO_2 which suppresses the nonuniform growth of microcrystals at the interfacial defects of Si,[11] which in turn leads to uniform amorphous SiO_2 with improved electric qualifies.

Acknowledgements

This study was performed under the approval of the National Laboratory for High Energy Physics (approval No. 94-Y12). We thank the staff at the Photon Factory for their convenience at the experiment.

1) N. Awaji, Y. Sugita, S. Ohkubo, T. Nakanishi, K. Takasaki and S. Komiya: Jpn. J. Appl. Phys. **34** (1995) L1013.
2) Y. Sugita, N. Awaji, S. Ohkubo, S. Watanabe, S. Komiya and T. Ito: *Ext. Abstr. Int. Conf. 1995 Solid State Devices & Materials Jpn.* (1995) p. 836.
3) S. Ohkubo, Y. Tamura, R. Sugino, T. Nakanishi, Y. Sugita, N. Awaji and K. Takasaki: *Proc. 1995 Symp. VLSI Tech. Dig. of Tech. Papers Jpn.* (1995) p. 111.
4) T. Nakanishi, Y. Sato, M. Okuno and K. Takasaki: *1994 Symp. VLSI Tech. Dig. of Tech. Papers* (1994) p. 45.
5) B. Vidal and P. Vincent: Appl. Opt. **23** (1984) 1794.
6) E. Hasegawa, A. Ishitani, K. Akimoto, M. Tsukiji and N. Ohta: J. Electrochem. Soc. **142** (1995) 273.
7) W. A. Pliskin: J. Vac. Sci. & Technol. **14** (1977) 1064.
8) S. Pantelides and M. Long: *Physics of* SiO_2 *& Its Interfaces*, ed. S. Pantelides (Pergamon, New York, 1978) p. 339.
9) A. M. Stoneham, C. R. M. Grovenor and A. Cerezo: Philos. Mag. **B55** (1987) 201.
10) V. A. Yakovlef, Q. Liu and E. A. Irene: J. Vac. Sci. & Technol. **A10** (1992) 742.
11) A. Ourmazd and J. Bevk: *Physics and Chemistry of* SiO_2 *& the* Si–SiO_2 *Interfaces*, eds. C. R. Helms and B. E. Deal (Plenum Press, New York, 1988) p. 189.
12) B. J. Mrstik, A. G. Revesz, M. Ancona and H. L. Hughes: J. Electrochem. Soc. **134** (1987) 2020.
13) I. Takahashi, T. Shimura and J. Harada: J. Phys., Condens. Matter **5** (1993) 6525.
14) I. Takahashi, K. Nakano, J. Harada, T. Shimura and M. Umeno: Surf. Sci. Lett. **315** (1994) L1021.